Mineralogy and Petrology (2006) 88: 207–226
DOI 10.1007/s00710-006-0156-2

Mineralogy and Petrology
Printed in Austria

Protolith and metamorphic ages of the Haiyangsuo Complex, eastern China: a non-UHP exotic tectonic slab in the Sulu ultrahigh-pressure terrane

J. G. Liou[1], **T. Tsujimori**[1], **W. Chu**[1], **R. Y. Zhang**[1], and **J. L. Wooden**[2]

[1] Department of Geological and Environmental Sciences, Stanford University, Stanford, California, U.S.A.
[2] U.S. Geological Survey, California, U.S.A.

Received September 9, 2005; accepted February 28, 2006
Published online August 8, 2006;
Editorial handling: A. Proyer

Summary

The Haiyangsuo Complex in the NE Sulu ultrahigh-pressure (UHP) terrane has discontinuous, coastal exposures of Late Archean gneiss with amphibolitized granulite, amphibolite, Paleoproterozoic metagabbroic intrusives, and Cretaceous granitic dikes over an area of about 15 km^2. The U–Pb SHRIMP dating of zircons indicates that the protolith age of a garnet-biotite gneiss is >2500 Ma, whereas the granulite-facies metamorphism occurred at around 1800 Ma. A gabbroic intrusion was dated at ~1730 Ma, and the formation of amphibolite-facies assemblages in both metagabbro and granulite occurred at ~340–460 Ma. Petrologic and geochronological data indicate that these various rocks show no evidence of Triassic eclogite-facies metamorphism and Neoproterozoic protolith ages that are characteristics of Sulu-Dabie HP-UHP rocks, except Neoproterozoic inherited ages from post-collisional Jurassic granitic dikes. Haiyangsuo retrograde granulites with amphibolite-facies assemblages within the gneiss preserve relict garnet formed during granulite-facies metamorphism at ~1.85 Ga. The Paleoproterozoic metamorphic events are almost coeval with gabbroic intrusions. The granulite-bearing gneiss unit and gabbro-dominated unit of the Haiyangsuo Complex were intruded by thin granitic dikes at about 160 Ma, which is coeval with post-collisional granitic intrusions in the Sulu terrane. We suggest that the Haiyangsuo Complex may represent a fragment of the Jiao-Liao-Ji Paleoproterozoic terrane developed at the eastern margin of the Sino-Korean basement, which was juxtaposed with the Sulu terrane prior to Jurassic granitic activity and regional deformation.

Introduction

Petrochemical and geochemical studies over the last decade have documented the world's largest Triassic ultrahigh-pressure (UHP) terrane between the Sino-Korean and Yangtze cratons in east-central China (e.g., *Zhang* et al., 1994; *Liou* et al., 1997a; *Hacker* et al., 2000). Numerous eclogites and subordinate garnet peridotites,

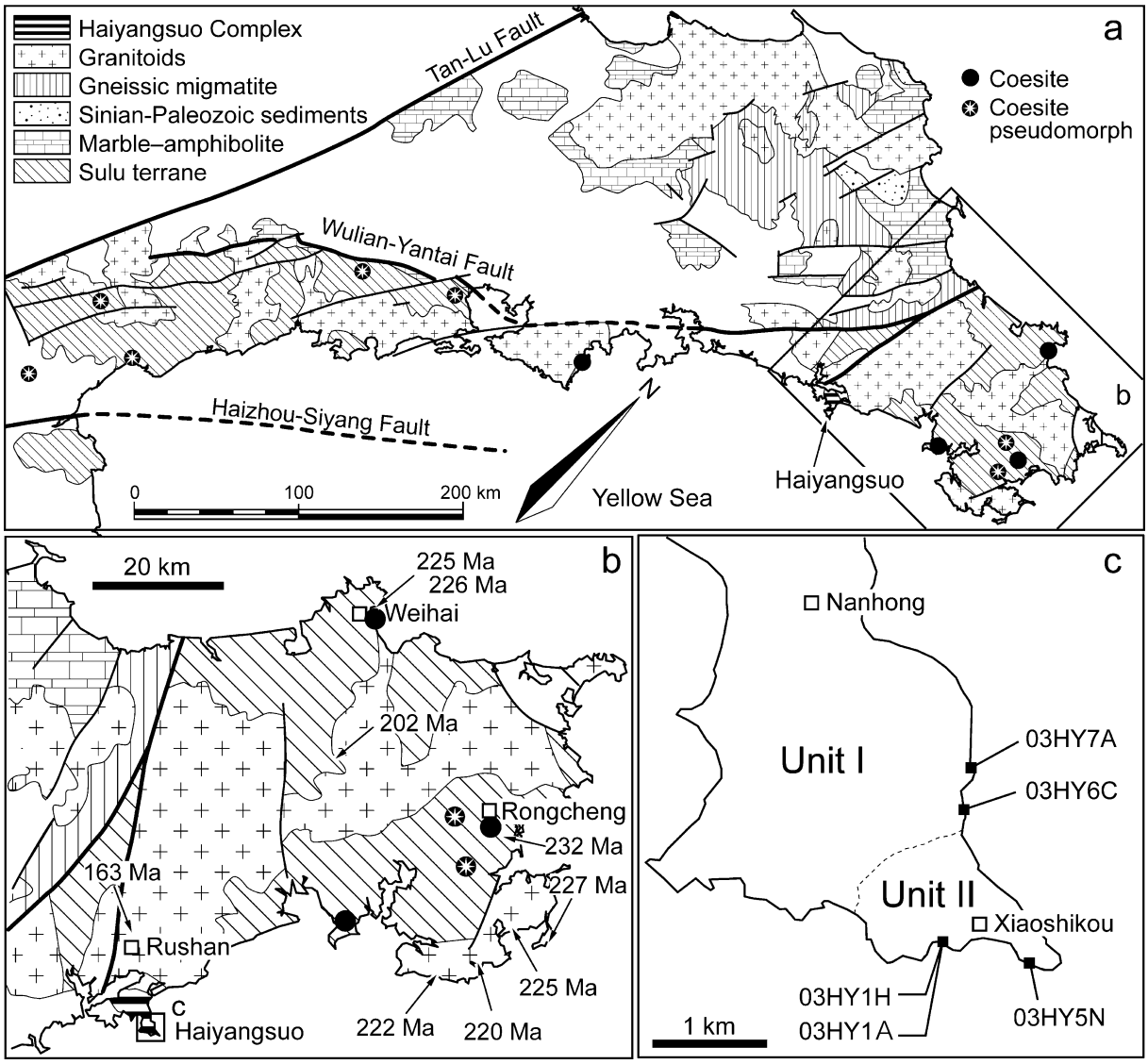

Fig. 1. **a** A simplified geologic map of the Shandong Peninsula, showing the distribution of major lithologic units, localities of coesite and coesite pseudomorphs (*Zhai* et al., 2000; *Yang* et al., 2003; *Zhang* et al., 1995), and the locality of the Haiyangsuo Complex (modified after *Faure* et al., 2003); **b** Schematic geological map of the eastern Shandong Peninsula, showing the location of the Haiyangsuo region, localities of coesite and coesite pseudomorphs, metamorphic age of UHP metamorphism and intrusion age of granitic pluton at Rushan. **c** Schematic geological map of the Haiyangsuo region in the Jiaodong Peninsula, showing distribution of 2 major rock units and sample localities

marbles, jadeite-quartzites and metapelites occur in country rock gneisses in this terrane. Petrological studies indicate that these rocks were subjected to *in-situ* UHP metamorphism during Triassic subduction of the Yangtze craton beneath the Sino-Korean craton (*Wang* and *Liou*, 1993; *Liu* et al., 2002; *Hirajima* and *Nakamura*, 2003). However, primary sedimentary and igneous structures including unconformity, pillow lava and gabbroic structures, and igneous minerals such as plagioclase, orthopyroxene and biotite have been documented in the Dabie-Sulu UHP terrane (*Hirajima* et al., 1993; *Zhang* and *Liou*, 1997; *Dong* et al., 2002; *Oberhänsli* et al., 2002; *Schmidt* et al., 2003). These relict structures and minerals were preserved in UHP rocks as fluid activities during the UHP and subsequent retrograde recrystallization are suggested to be extremely low (e.g., for detailed summary see *Jahn* et al., 2003; *Rumble* et al., 2003; *Zheng* et al., 2003). However, non-UHP orthogneisses were recently documented from 1100 metre continuous drill cores based on detailed examinations of mineral inclusions in zircon separates from these gneissic rocks (*Liu* et al., 2002). The Chinese Scientific Drilling site in Donghai, SW Sulu is about 300 km southwest of the studied region in Haiyangsuo.

The Haiyangsuo Complex (HYC) in NE Sulu (Fig. 1) contains massive bodies and thin dikes of amphibolitized metagabbro discontinuously occurring in country rock felsic gneiss along the coast over an area of about 15 km^2. Our petrologic investigations indicate that no coesite, omphacite or other UHP index minerals occurs in either gneiss or metagabbro and no eclogite-facies assemblage has been documented in this region (*Liou* et al., 1997b; *Chu*, 2005; *Zhang* et al., 2006). Is the absence of UHP index minerals and eclogite-facies assemblage due to the lack of fluid activity suggested above, or is the HYC an exotic terrane from the Sulu (e.g., *Liou* et al., 1997b)?

We address this question through the U–Pb SHRIMP dating of zircons from representative rocks in the HYC. If the zircon separates from granulite, metagabbro and gneissic rocks do not yield Triassic metamorphic ages nor Neoproterozoic protolith ages, the HYC must have experienced a different *P*–*T*–t evolution than adjacent Sulu UHP rocks. If the HYC is not part of the Sulu UHP-HP terrane, a tectonic contact must occur between the two terranes. In addition, the boundary and the size of the Sulu UHP terrane must be redefined in order to better constrain the modeling of the exhumation process in the UHP terrane.

Preliminary geochronological data of the HYC rocks are included in *Chu* (2005). Mineral abbreviations are after *Kretz* (1983) and the term 'hornblende (Hbl)' is used to describe Ca-amphibole with dominantly pargasitic, tschermakitic and edenitic compositions throughout this paper.

Geologic outline

The Haiyangsuo region situated to the south of Rushan County in the Shandong Peninsula at the northeastern end of the Sulu UHP terrane is part of the Paleo- to Mesoproterozoic Jiaodong group (*Li* et al., 1994) (Fig. 1a, b). Along the coast, amphibolites and metagabbros and their enclosing gneissic rocks of the HYC are widely exposed. *Ye* et al. (1999) describe granulite relics within amphibolite displaying garnet coronas between plagioclase and mafic minerals. They named such rock with the assemblage of Grt + Cpx ($Jd_{<22}$) + Pl + Zo + Hbl + Ky + Rt a

''transitional eclogite.'' They further suggested that the HYC could be correlated with the ''cold eclogite'' belt in Dabie, and represents a southern HP belt of the Sulu UHP metamorphic terrane. As granulite-facies protoliths are rare for Dabie-Sulu UHP rocks, their findings motivated us to investigate the lithology, P–T paths and geochronology of the Haiyangsuo rocks. Our results for parageneses and compositions of minerals from granulite, amphibolite and metagabbro and P–T paths are presented in *Zhang* et al. (2006).

A small peninsula to the south of Nanhong can be subdivided into two map units (Fig. 1c): a granulite-bearing gneiss unit (Unit I), and a metagabbro-dominated unit (Unit II). Both units are cross-cut by granitic dikes. Since this area is flat and heavily farmed, the lithologic characteristics and contact relations of these units were observed only along the coast.

Granulite-bearing gneiss (Unit I)

This unit is most abundant and consists of over 90% felsic gneiss with less than 10% mafic rocks. The gneiss shows distinct compositional layers of various thicknesses (Fig. 2a); some layers show pinch-and-swell structures and are refolded, and others are homogeneous and massive. Poly-phase deformation with tight to isoclinal folds is characteristic of this unit. At least two stages of deformation were identified. Felsic dikes cross-cutting both gabbroic intrusives and the host gneiss are apparent in many outcrops. Dark, garnet-free amphibolite layers are concordant with the host gneiss. Minor granulite layers were identified in this unit; these include biotite-bearing two-pyroxene granulite, pargasite-bearing two-pyroxene mafic granulite, and garnet clinopyroxenite (see *Zhang* et al., 2006, for detailed descriptions). All granulites are weakly deformed and variably retrogressed. Parageneses and compositions of minerals from mafic granulites indicate these mafic layers record two distinct stages of metamorphic recrystallization: (a) an early HP granulite-(Grt + Opx + Cpx + Pl + Hbl [pargasitic] + Rt/Ilm) to amphibolite-facies metamorphism and (b) a later amphibolite-facies overprint (Pl + Hbl ± Grt + Ttn ± Ep ± Qtz) (*Zhang* et al., 2006). In some samples, the later amphibolite-facies paragenesis is characterized by fine-grained (0.05–0.1 mm) garnet coronas along grain boundaries between plagioclase and pyroxene or between earlier porphyroblastic garnet and pyroxene.

Metagabbro-dominated unit (Unit II)

The southwestern part of the peninsula is covered by one undifferentiated unit consisting of more than 60% amphibolitized gabbroic intrusives and about 40% rocks of gneissic Unit I. Along the coast near Xiaoshikou (Fig. 1), both gneiss and metagabbro are well exposed (Fig. 2). The field relations of gneiss and metagabbroic intrusives can be easily observed: metagabbro discordantly intruded into gneiss. The metagabbros occur as discontinuous bodies of less than 1 metre to more than 50 metre size, and are most common in the Xiaoshikou region. Some metagabbroic dikes cross-cut the gneiss and show distinct chilled margins; others are concordant with the foliation of gneissic units and are difficult to differentiate from amphibolite layers.

Gabbroic rocks exhibit various extents of amphibolite-facies recrystallization (for details see *Zhang* et al., 2006). Fine-grained pale reddish coronal metagabbro

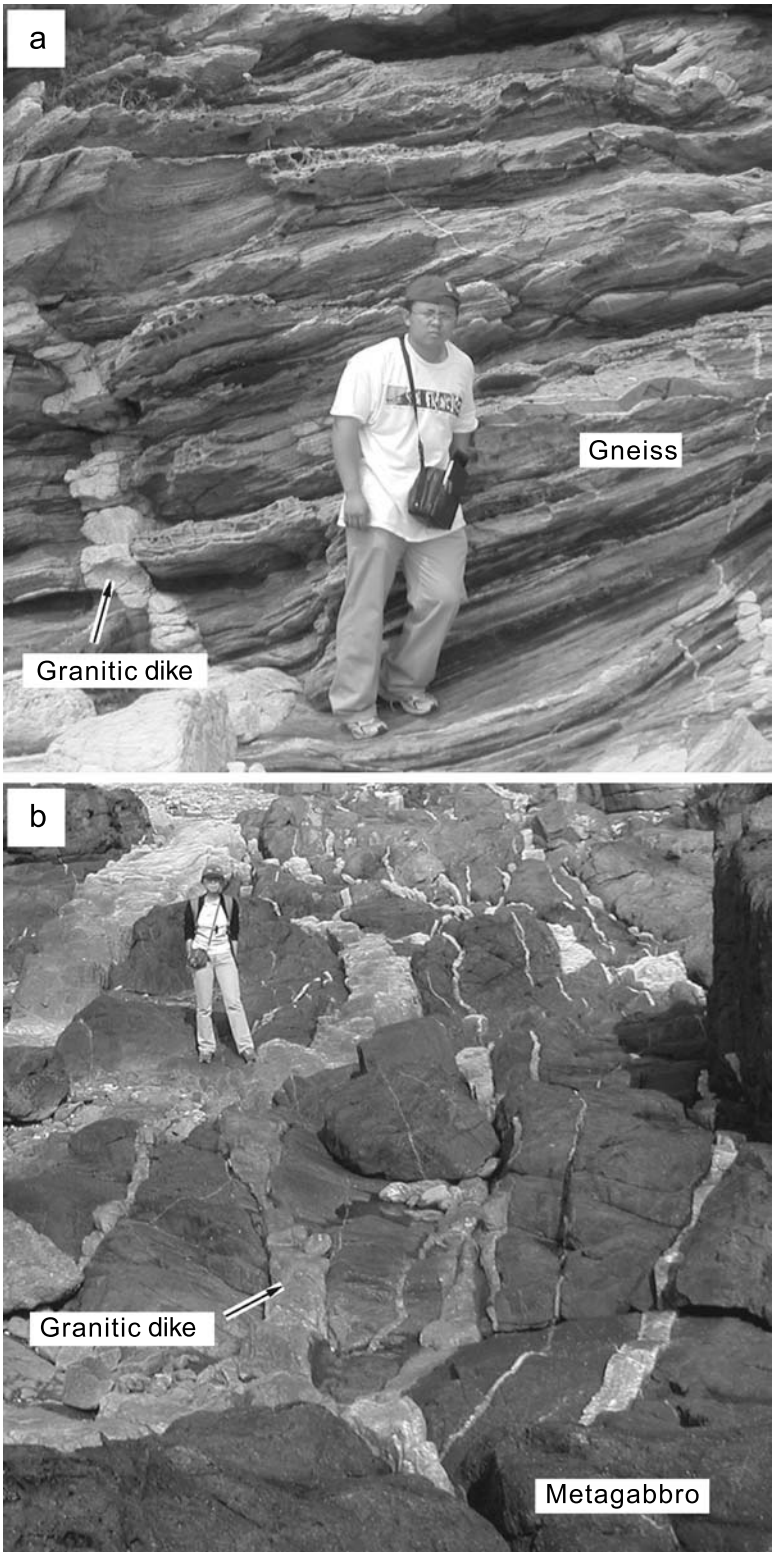

Fig. 2. Photographs showing field view. **a** Banded gneiss of Unit I cross-cut by granitic dike; **b** massive amphibolitized metagabbro of Unit II cross-cut by various granitic dikes

occurs at the core of metagabbro bodies or in the central part of mafic dikes. Coronal metagabbro contains relict igneous minerals, Opx + Cpx + Pl + Amp + Ilm ± Qtz; the common sequences of corona layers between pyroxene and plagioclase are Cpx (or Opx) | Amp_2 + Qtz | Grt | Pl_2 with zoisite and kyanite needles, or Opx | Amp_2 + Qtz + Di | Ab | Grt | Pl_2 with zoisite and kyanite. Coronal metagabbro is easily misidentified as fine-grained eclogite because of its reddish color and the presence of garnet and clinopyroxene. Reddish metagabbro cores vary in size; most range from 1 to 10 metre in diameter. Toward the margins of mafic bodies, the rock color gradually changes to dark green due to amphibolite-facies recrystallization.

Granitic dikes

Granitic dikes cross-cut both Units I and II (Fig. 2). These granitic dikes have thickness of decimetres to metres and contain K-feldspar, quartz and plagioclase. Some K-feldspar grains are extremely coarse (up to 4 cm) and pink in color. Euhedral coarse-grained garnet is also present in some granitic rocks. At some outcrops, granitic dikes are highly deformed and show mylonitic texture.

Previous geochronologic studies

Although the Haiyangsuo region has been considered to be part of the Sulu terrane (e.g., *Regional Geology of Shandong Province*, 1991), only a few geochronological studies are available. *Li* et al. (1994) reported conventional U–Pb ages of zircons in amphibolites from this region. Zircon xenocrysts of their samples gave a weighted mean age of 2149 Ma and magmatic euhedral zircons yielded an upper intercept age of 1784 ± 11 Ma. They interpreted the lower intercept age of 448 ± 13 Ma as the result of lead loss. *Wallis* et al. (2005) dated a strongly deformed K-feldspar-rich dike in this region. Seven U–Pb SHRIMP analyses of zircon yield a wide range of $^{206}Pb/^{238}U$ ages, 155.2–755.7 Ma. Although they suggested that these dikes originated from partial melts of the dominant felsic Sulu gneiss at 200–230 Ma, these analyses in the Tera-Wasserburg concordia diagram did not yield a meaningful weighted mean $^{206}Pb/^{238}U$ age or define a regression trend. *Zhang* et al. (2006) dated a mafic HP granulite from Unit I. Their zircon U–Pb SHRIMP ages yielded an upper intercept age of 1846 ± 26 Ma and a lower intercept age of 373 ± 65 Ma.

Petrologic characteristics of dated samples

In this study, representative rocks were carefully selected for dating on the basis of detailed petrogeneses and *P–T* estimates (*Chu*, 2005; *Zhang* et al., 2006). Gneiss and retrograde granulite from Unit I, and a metagabbro, an amphibolite and a granitic dike from Unit II were dated. All samples were collected at outcrops along the coast; sample localities are shown in Fig. 1c.

Gneiss of Unit I (sample 03HY7A)

Sample 03HY7A is a quartz-rich biotite-garnet gneiss consisting mainly of quartz, biotite, and subordinate amounts of garnet and plagioclase with minor muscovite

and rutile. Monazite and apatite occur as accessory minerals. Garnet porphyroblasts (<5 mm) contain inclusions of quartz, rutile and rare biotite. Matrix rutile is partly rimmed by ilmenite. The mineral assemblage Qtz + Pl + Bt + Grt ± Rt + Ilm suggests amphibolite-facies conditions.

Retrograde granulite of Unit I (sample 03HY6C)

Sample *03HY6C* is the retrograded equivalent of a mafic HP granulite (03-R14) described by *Zhang* et al. (2006). Although relict garnet and brown pargasitic hornblende are locally preserved as porphyroblasts, clinopyroxene is completely replaced by fine-grained aggregates of greenish hornblende; plagioclase is also replaced by fine-grained aggregates of zoisite/clinozoisite. The assemblage Grt (relic) + brown Hbl (relic) + "Cpx" pseudomorph + "Pl" pseudomorph + Rt + Qtz characterizes the granulite-facies stage. In contrast, the assemblage green Hbl + Grt + Zo/Czo + Qtz represents the amphibolite-facies overprint; coronitic garnet occurs at grain boundaries of relict granulite-facies minerals. *Zhang* et al. (2006) estimated $T > 750\,^{\circ}C$ and $P = 0.9$–1.1 GPa for the granulite-facies stage and suggested a nearly isobaric P–T trajectory to regional amphibolite-facies metamorphism.

Metagabbro of Unit II (sample 03HY1H)

Sample 03HY1H is a partially amphibolitized metagabbro preserving the original mineral assemblage of noritic gabbro, brown Hbl (relic) + "Pl" pseudomorph + "Cpx" pseudomorph ± "Opx" pseudomorph + Ilm. These igneous relics are partly replaced by greenish hornblende, rare cummingtonite and zoisite/clinozoisite; coronitic garnet occurs along grain boundaries of primary igneous phases; the assemblage green Hbl + Grt + Zo/Czo + Qtz represents amphibolite-facies recrystallization.

Amphibolitic layer of Unit II (sample 03HY1A)

Sample 03HY1A is from a concordant amphibolitic layer within biotite-garnet gneiss. It consists mainly of greenish hornblende, plagioclase and quartz with minor epidote, biotite, and titanite. The assemblage Hbl + Pl + Qtz + Ep + Bt + Ttn represents amphibolite-facies recrystallization.

Granitic dike of Unit II (sample 03HY5N)

Sample 03HY5N is a strongly deformed granitic dike showing mylonitic texture; porphyroclasts (8 mm) of K-feldspar, plagioclase and quartz occur in fine-grained matrix consisting mainly of recrystallized quartz (<0.2 mm).

Zircon U–Pb geochronology

Analytical methods

U–Th–Pb analyses were performed with the SHRIMP-RG in the USGS-Stanford Ion Probe Laboratory. Instrumental conditions and data acquisition are similar to

Table 1. *Ion-probe U–Th–Pb isotope data of zircon in major rock types of the Haiyangsuo Complex*

	U (ppm)	Th (ppm)	Th/U	Rad. ^{206}Pb	Comm. ^{206}Pb (%)	$^{206}Pb/^{238}U$	error (%)	$^{207}Pb/^{206}Pb$	error (%)	$^{207}Pb/^{206}Pb$ age (Ma)	error	$^{206}Pb/^{238}U$ age (Ma)	error
Gneiss (3HY7A) of Unit I													
7A-1	643	362	0.58	197	−0.011	0.357	0.891	0.150	0.443	2347	7.6	1967	15.1
7A-2	218	6	0.03	58	0.019	0.307	1.006	0.111	0.882	1824	16.0	1727	15.2
7A-3	2129	543	0.26	789	0.040	0.432	0.866	0.154	0.370	2395	6.3	2313	16.8
7A-4	1885	55	0.03	67	0.586	0.041	0.880	0.053	2.059	333	46.7	260	2.2
7A-5	1301	21	0.02	462	0.000	0.413	0.858	0.149	2.224	2331	38.1	2229	16.2
7A-6	335	304	0.94	33	0.282	0.113	0.995	0.091	1.401	1445	26.7	689	6.5
7A-7	678	24	0.04	189	0.016	0.325	0.889	0.113	0.674	1856	12.2	1816	14.1
7A-8	774	351	0.47	105	0.043	0.159	0.892	0.105	0.550	1708	10.1	949	7.9
7A-9	206	106	0.53	56	0.043	0.315	1.083	0.147	1.134	2308	19.5	1764	16.7
7A-10	497	39	0.08	118	0.000	0.276	0.915	0.108	0.572	1771	10.4	1572	12.8
7A-11	379	116	0.32	152	0.000	0.466	0.929	0.172	0.363	2580	6.1	2465	19.0
7A-12	222	103	0.48	17	0.548	0.087	1.091	0.066	2.546	817	53.2	537	5.6
7A-13	624	294	0.49	182	0.013	0.339	0.894	0.141	0.541	2245	9.4	1884	14.6
7A-14	772	104	0.14	312	0.011	0.470	0.894	0.163	3.592	2489	60.5	2485	18.4
7A-15	1746	60	0.04	343	0.011	0.228	0.863	0.102	2.370	1666	43.9	1326	10.3
7A-16	100	89	0.92	35	0.102	0.405	1.265	0.159	1.889	2449	32.0	2190	23.5
7A-17	298	129	0.45	130	0.018	0.507	0.992	0.169	0.797	2549	13.3	2642	21.5
7A-18	534	329	0.64	127	0.038	0.277	0.933	0.136	0.785	2172	13.7	1574	13.0
7A-19	271	121	0.46	46	−0.043	0.198	0.998	0.118	1.276	1932	22.9	1165	10.6
7A-20	3899	82	0.02	1140	0.009	0.340	0.933	0.113	0.177	1850	3.2	1888	15.3
7A-21	471	233	0.51	143	−0.012	0.353	0.911	0.145	1.046	2282	18.0	1950	15.3
7A-22	476	109	0.24	194	0.000	0.474	0.938	0.173	1.354	2591	22.6	2502	19.4
7A-23	209	47	0.24	60	0.019	0.334	1.068	0.115	0.682	1874	12.3	1856	17.2
7A-24	1077	589	0.56	265	0.236	0.286	0.878	0.142	0.499	2249	8.6	1620	12.6
7A-25	528	22	0.04	180	0.017	0.396	0.902	0.135	1.725	2169	30.1	2149	16.5
7A-26	258	4	0.02	76	0.034	0.342	0.977	0.112	1.210	1833	21.9	1896	16.1
7A-27	686	164	0.25	279	0.022	0.472	0.885	0.181	0.486	2660	8.1	2494	18.3
Retrograde granulite (3HY6C) of Unit I													
6C-1	70	18	0.26	176	0.141	0.294	0.726	0.109	1.284	1787	23.4	1661	10.6
6C-2	29	8	0.28	197	0.000	0.080	1.723	0.074	4.506	1042	90.9	497	8.2
6C-3	2386	744	0.32	361	0.003	0.176	0.169	0.096	1.040	1546	19.5	1046	1.6
6C-4	37	7	0.21	911	0.693	0.284	1.059	0.103	2.903	1682	53.6	1611	15.1
6C-5	1711	306	0.18	554	0.039	0.038	0.247	0.053	0.844	311	19.2	238	0.6
6C-6	31	6	0.20	287	0.694	0.107	1.356	0.077	5.224	1132	104	656	8.5
6C-7	1077	166	0.16	129	−0.002	0.139	0.266	0.086	0.460	1349	8.9	840	2.1
6C-8	1594	282	0.18	433	0.000	0.316	0.194	0.114	1.817	1863	32.8	1770	3.0
6C-9	1311	224	0.18	277	0.022	0.246	4.130	0.110	3.936	1799	71.6	1419	52.6
6C-10	29	5	0.19	354	0.000	0.140	1.255	0.094	2.441	1507	46.1	844	9.9
6C-11	234	30	0.13	661	0.033	0.329	0.439	0.114	0.786	1857	14.2	1835	7.0
6C-12	1353	238	0.18	306	0.010	0.263	0.587	0.106	1.232	1728	22.6	1504	7.9
6C-13	30	8	0.27	642	0.000	0.253	1.098	0.105	1.712	1712	31.5	1455	14.3
6C-14	29	5	0.18	736	0.000	0.291	1.102	0.112	1.725	1835	31.3	1646	16.0

(*continued*)

Table 1 (*continued*)

	U (ppm)	Th (ppm)	Th/U	Rad. ^{206}Pb	Comm. ^{206}Pb (%)	$^{206}Pb/^{238}U$	error (%)	$^{207}Pb/^{206}Pb$	error (%)	$^{207}Pb/^{206}Pb$ age (Ma)	error	$^{206}Pb/^{238}U$ age (Ma)	error
6C-15	275	46	0.17	375	0.003	0.159	1.383	0.095	0.800	1529	15.1	949	12.2
6C-16	1625	287	0.18	401	0.004	0.287	0.576	0.108	0.864	1769	15.8	1626	8.3
6C-17	1497	352	0.24	391	0.019	0.304	0.321	0.112	1.096	1830	19.9	1711	4.8
6C-18	36	19	0.55	749	0.155	0.244	1.167	0.107	1.679	1753	30.7	1409	14.8
6C-19	36	8	0.22	997	−0.228	0.320	0.990	0.120	1.594	1955	28.5	1791	15.5
6C-20	184	65	0.36	354	0.127	0.223	0.484	0.104	0.837	1700	15.4	1299	5.7
6C-21	179	20	0.12	407	0.065	0.265	0.821	0.105	0.707	1719	13.0	1513	11.1
6C-22	191	80	0.43	551	0.035	0.336	0.485	0.114	0.811	1862	14.6	1867	7.9
6C-23	2839	635	0.23	786	0.000	0.322	2.090	0.109	1.133	1783	20.7	1801	32.8
6C-24	79	12	0.16	231	1.660	0.034	1.446	0.049	16.421	143	385	214	3.0
6C-25	2101	302	0.15	191	0.007	0.106	2.015	0.084	2.815	1296	54.7	649	12.4
6C-26	35	6	0.19	724	0.031	0.237	1.030	0.107	1.665	1742	30.5	1373	12.7
6C-27	1875	379	0.21	514	0.008	0.319	0.711	0.113	1.121	1841	20.3	1786	11.1
6C-28	2299	587	0.26	275	0.016	0.139	0.285	0.099	5.794	1609	108	840	2.2
Metagabbro (3HY1H) of Unit II													
1H-1	227	43	0.20	181	0.110	0.093	0.499	0.063	1.539	719	32.7	574	2.7
1H-2	308	306	1.03	804	0.031	0.304	0.390	0.106	0.503	1731	9.2	1711	5.9
1H-3	689	990	1.49	183	0.015	0.309	0.234	0.106	0.326	1727	6.0	1738	3.6
1H-4	1284	1312	1.06	341	0.018	0.309	0.186	0.106	0.359	1734	6.6	1737	2.8
1H-5	909	1012	1.15	213	0.014	0.273	0.237	0.105	0.358	1719	6.6	1557	3.3
1H-6	520	633	1.26	136	0.002	0.305	0.264	0.106	0.376	1740	6.9	1716	4.0
1H-7	147	225	1.58	213	0.000	0.169	0.601	0.096	0.976	1542	18.4	1004	5.6
1H-8	2651	3310	1.29	710	0.000	0.312	0.148	0.106	0.217	1730	4.0	1749	2.3
1H-9	647	557	0.89	164	0.032	0.294	0.370	0.106	0.356	1733	6.5	1663	5.4
1H-10	321	346	1.12	806	0.000	0.293	0.714	0.106	0.482	1723	8.9	1655	10.4
Amphibolitic layer (3HY1A) of Unit II													
1A-1	686	770	1.16	183	0.029	0.311	0.893	0.106	0.417	1726	7.7	1745	13.7
1A-2	80	38	0.49	11	0.205	0.162	1.323	0.096	1.770	1539	33.3	965	11.9
1A-3	528	469	0.92	129	0.026	0.285	0.909	0.104	0.486	1702	9.0	1615	13.0
1A-4	67	28	0.43	8	1.194	0.133	1.441	0.087	4.320	1365	83.2	804	10.9
1A-5	728	711	1.01	191	0.032	0.306	0.887	0.106	0.396	1731	7.3	1721	13.4
1A-6	411	339	0.85	101	0.057	0.287	0.933	0.104	0.561	1705	10.3	1625	13.4
1A-7	365	155	0.44	26	0.389	0.082	1.006	0.075	2.014	1067	40.5	509	4.9
1A-8	129	73	0.59	34	0.059	0.304	1.135	0.105	0.987	1707	18.2	1710	17.0
1A-9	101	49	0.50	24	0.227	0.279	1.194	0.105	1.228	1708	22.6	1588	16.8
1A-10	177	104	0.61	45	0.025	0.296	1.052	0.105	0.823	1710	15.1	1669	15.5
1A-11	153	89	0.60	37	0.042	0.281	1.080	0.105	0.908	1713	16.7	1596	15.3
1A-12	677	743	1.13	168	0.011	0.289	0.892	0.105	0.423	1719	7.8	1636	12.9
1A-13	837	819	1.01	219	0.020	0.305	0.879	0.106	0.367	1733	6.7	1717	13.2
1A-14	827	789	0.99	209	−0.019	0.294	0.879	0.106	0.380	1736	7.0	1660	12.9
1A-15	164	78	0.49	43	0.037	0.302	1.066	0.105	1.327	1709	24.4	1702	15.9
1A-16	364	291	0.83	96	0.068	0.307	0.943	0.106	0.578	1739	10.6	1726	14.3

(*continued*)

Table 1 (*continued*)

	U (ppm)	Th (ppm)	Th/U	Rad. ^{206}Pb	Comm. ^{206}Pb (%)	^{206}Pb/^{238}U	error (%)	^{207}Pb/^{206}Pb	error (%)	^{207}Pb/^{206}Pb age (Ma)	error	^{206}Pb/^{238}U age (Ma)	error
1A-17	135	84	0.64	25	−0.013	0.217	1.133	0.100	1.138	1622	21.2	1265	13.0
1A-18	458	384	0.87	121	0.051	0.308	0.921	0.105	0.502	1723	9.2	1733	14.0
1A-19	522	399	0.79	99	0.028	0.220	0.915	0.103	0.638	1680	11.8	1281	10.6
1A-20	112	61	0.57	28	0.107	0.294	1.155	0.105	1.129	1720	20.7	1661	16.9
Granitic dike (3HY5N) of Unit III													
5N-1	197	146	0.77	19.0	0.092	0.112	1.111	0.062	1.851	676	39.6	685	7.2
5N-2	248	155	0.65	27.3	0.138	0.128	1.042	0.063	1.689	714	35.9	777	7.6
5N-3	199	166	0.86	10.2	0.804	0.059	1.253	0.053	5.928	337	134	372	4.5
5N-4	173	139	0.83	12.7	0.452	0.085	1.163	0.058	2.880	546	62.9	527	5.9
5N-5	185	218	1.22	9.7	0.688	0.061	1.213	0.055	4.752	427	106	381	4.5
5N-7	738	7	0.01	21.9	0.109	0.034	0.973	0.052	1.854	270	42.5	218	2.1
5N-8	43	22	0.52	4.1	0.544	0.111	1.709	0.059	3.934	581	85.4	677	11.0
5N-9	189	107	0.59	15.3	0.074	0.095	1.116	0.064	1.878	733	39.8	583	6.2
5N-11	893	243	0.28	43.7	0.062	0.057	0.914	0.058	1.176	537	25.7	357	3.2
5N-14	518	276	0.55	50.2	0.105	0.113	0.931	0.065	1.254	758	26.4	688	6.1
5N-15	474	78	0.17	10.1	0.225	0.025	1.114	0.048	5.169	120	122	158	1.7
5N-16	63	32	0.53	6.3	0.893	0.117	1.508	0.057	5.047	498	111	711	10.2
5N-17	2218	526	0.24	48.6	0.807	0.025	0.899	0.047	3.254	50	77.7	161	1.4
5N-18	934	118	0.13	19.8	0.117	0.025	0.969	0.049	2.008	141	47.1	157	1.5

All errors are 1 sigma of standard deviation; error in standard calibration was 0.19% (not included in above errors)
A negative value indicates that the number of ion counts was indistinguishable from background; in such case no common Pb correction is made
* Percentage of common ^{206}Pb in total measured ^{206}Pb; common Pb corrected using measured ^{204}Pb

those described by *Williams* (1998). Analytical spots, ~40 μm in diameter, were sputtered using an ~5 nA O_2^- primary beam. The data were collected in sets of six scans through 9 mass spectra. The primary beam was rastered across the analytical spot for 120 seconds before analysis to reduce surficial common Pb resulting from sample preparation and Au-coating. Concentration data were calibrated against CZ3 zircon (550 ppm U), and isotope ratios were calibrated against zircon R33 (419 Ma, *Black* et al., 2004). Data reduction followed *Williams* (1998), and utilized the Squid software (*Ludwig*, 2001). Isoplot 3 (*Ludwig*, 2003) was used to calculate all ages, which are reported here at the 95% confidence level. Cathodoluminescence (CL) images were obtained using a JEOL 5600LV Scanning Electron Microscope (SEM) equipped with a HAMAMATSU photo multiplier tube. The dating results are summarized in Table 1.

Zircon morphology and internal texture

Zircon separates (~50–200 μm) from Unit I gneiss (03HY7A) have rounded and stubby morphology and exhibit internal structures. Most crystals have thick cores exhibiting oscillatory zoning mantled by extremely thin rims (Fig. 3a). These rims

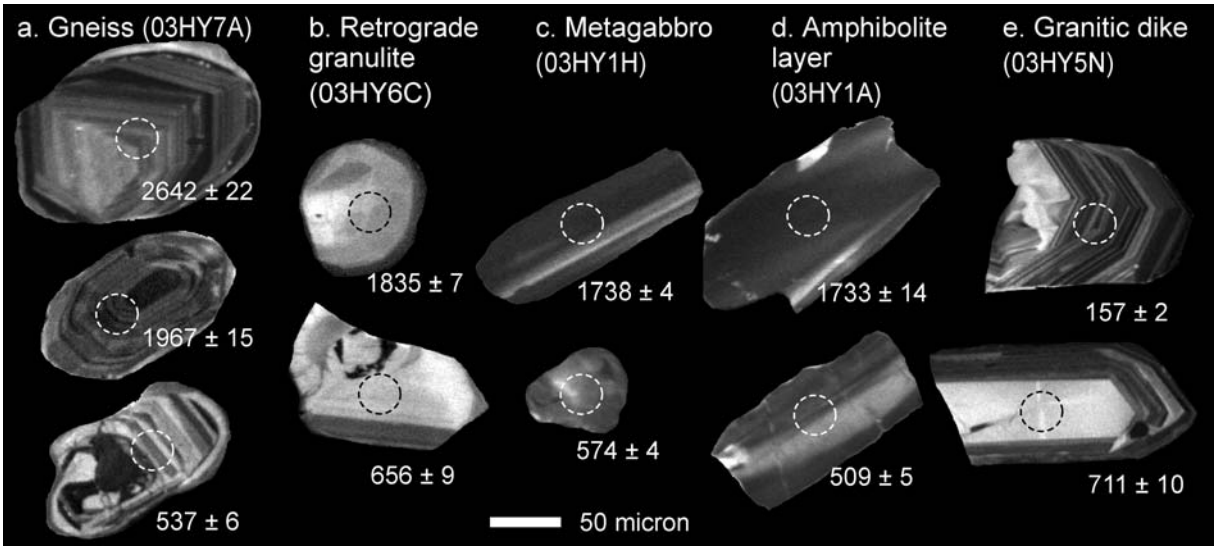

Fig. 3. Cathodoluminescence image of representative zircon separates from various rock types of the Haiyangsuo Complex. Ellipses within crystal represent primary beam pits for SHRIMP dating

have highly luminescent and homogeneous CL colors characteristic for metamorphic zircons.

Zircon separates (~100–300 μm) from retrograde granulite of Unit I (03HY6C) have relatively smooth and elliptical to rounded shapes (Fig. 3b). Cores are highly luminescent. The internal growth structure is characterized by a faintly patchy pattern.

Zircon separates (~30–100 μm) from metagabbro (03HY1H) and amphibolitic layer (03HY1A) of Unit II do not show obvious internal zoning (Fig. 3c and d). However, most zircon grains show strips of different luminescence characteristic for zircons of mafic rocks.

Zircon separates (~50–300 μm) from granitic dike of Unit II (03HY5N) show distinct inherited cores and oscillatory zoned rims. They have prismatic and euhedral shape, clearly exhibiting the internal growth zoning of magmatic origin in outer domains (Fig. 3e); these textures suggest the granitic melt may have resulted from partial melting of gneissic rocks.

Th–U chemistry of zircons

Th and U concentrations of zircon crystals are shown in Fig. 4. Zircons from gneiss of Unit I (03HY7A) have highly variable Th/U ratios, spanning a range of 2 orders of magnitude. Zircons from retrograde granulite of Unit I (03HY6C) have constant Th/U ratios with an average value of about 0.3. Zircons of metagabbro (03HY1H) and amphibolitic layer (03HY1A) of Unit II have constant Th/U ratios around the value of 1 except for some analyses with lower Th/U ratio. In the granite dike of Unit II (03HY5N), igneous rims have lower Th/U ratios (<0.35) than the cores.

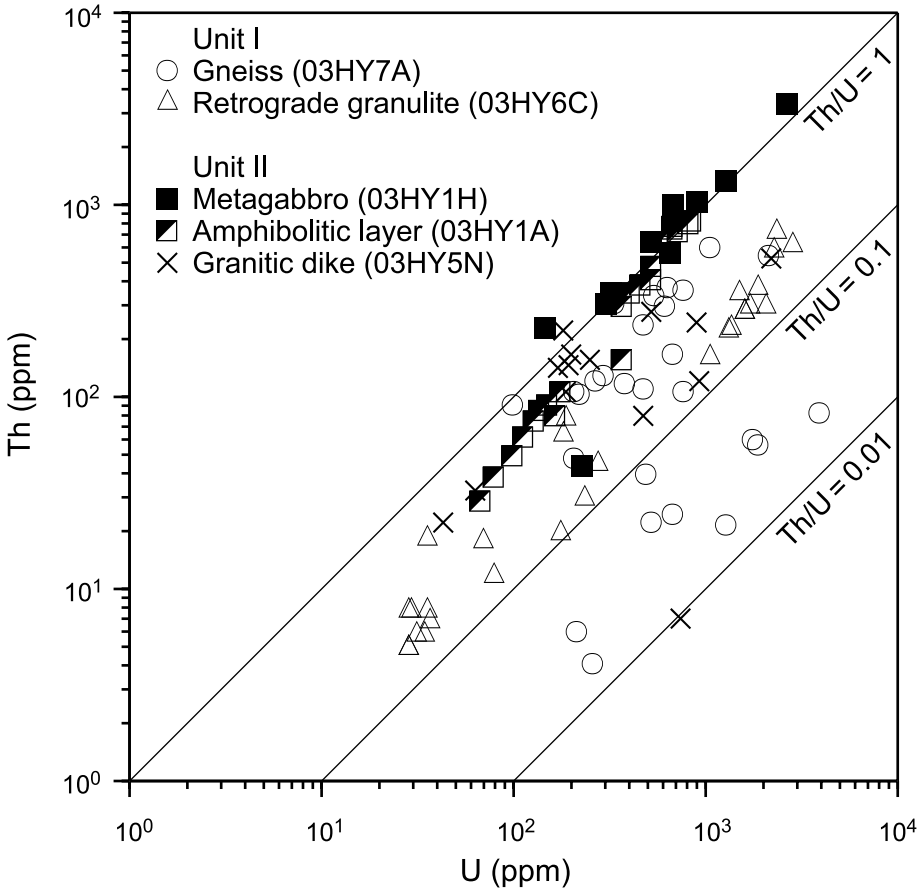

Fig. 4. Th and U abundance (ppm) of zircon spots analyzed by SHRIMP. For explanation see text

Age of inherited zircon and older metamorphism

In the gneiss of Unit I (03HY7A), the group of the oldest apparent $^{207}Pb/^{206}Pb$ ages has a mean value >2500 Ma (Fig. 5, Table 1), which is the oldest age obtained in the HYC. In terms of the whole sample, apparent ages scatter largely in excess of their analyses, thus, the U–Pb system of zircons became complex by one to several of the following mechanisms: multiple growth of new zircon, multiple episodic Pb-loss events, and partially continuous Pb-loss. It is observed that in the upper part, the zircon data are concordant or very close to the concordia (Fig. 5a). A mixing line is drawn to fit these near concordant data. The upper intercept might represent the protolith age of about 2650 Ma. The lower intercept of the mixing line yields an age of about 1800 Ma; this age may represent the first metamorphic event. *Li* et al. (1994) suggested that a gabbroic intrusive event at about 1800 Ma might be coeval with this metamorphic event.

Some data of the present study were found to be grossly discordant. To fit all these discordant points, Pb-loss lines can be drawn starting from the mixing line. It seems that all the Pb-loss lines converge and lead to an age of about 600 Ma. Because this Archean gneiss could be affected by several thermal events, hence

more than one Pb-loss events, no unique lower-intercept ages were obtained. Multiple-stage Pb-loss can account for the complexity of the concordia diagram, therefore the lower-intercept age of 600 Ma may be geologically meaningless.

Most zircon data of the retrograde granulite of Unit I (03HY6C) are discordant, indicating significant Pb loss (Fig. 5b); such an effect may have resulted in large analytical errors for this sample shown in Table 1. The early Proterozoic age is similar to the age of 1846 ± 26 Ma obtained by *Zhang* et al. (2006) on another granulite sample (03-R14) from the same locality; they may correspond to the HP granulite-facies growth of zircon grains. The lower-intercept age overlaps on errors of the lower-intercept age of 373 ± 65 Ma for a less retrograde granulite from the same locality (for details see *Zhang* et al., 2006). Although these lower-intercept ages have large error ranges, these Paleozoic ages may represent the timing of amphibolite-facies overprint when the fine-grained secondary garnet corona formed.

In Unit II, the metagabbro (03HY1H) cross-cuts Unit I gneiss, hence has a younger age. *Li* et al. (1994) suggested that the gabbroic intrusion occurred during the granulite- to amphibolite-facies metamorphic event producing gneiss and granulite. The concordia diagram for 03HY1H has upper and lower intercept ages of 1734.2 ± 5.1 and 339 ± 59 Ma, respectively (MSWD = 1.5) (Fig. 5c). Most zircon data are near concordant at 1650–1750 Ma. Only two spots show very obvious Pb-loss of up to 55 percent. It is likely that gabbroic magma intruded regionally in the HYC at about 1730 Ma. This event may have been coeval with regional amphibolite-facies metamorphism of late Archean/early Proterozoic granulite-bearing gneissic terranes as indicated in Fig. 5a. The lower intercept ages imply that a second regional amphibolite-facies metamorphic event occurred in this region in the middle Paleozoic.

The amphibolitic layer of Unit II (03HY1A) has an upper intercept age of 1731 ± 6 Ma, representing the intrusive age of gabbroic magma (Fig. 5d). On the other hand, the lower intercept age of 338 ± 28 Ma is identical to the metamorphic age of metagabbro 03HY1H mentioned above, indicating that the second regional amphibolite-facies metamorphic event affected all older rocks including gneiss, granulite and gabbroic intrusive. All the zircon data fit the discordant line well. Most zircons did not experience significant Pb-loss; they are very close to concordia within the range of 1600–1800 Ma. Five zircon data show obvious Pb-loss and lie on the discordant line.

Age of youngest granitic intrusions

As described above, distinct metamorphic core and magmatic oscillatory overgrowths can be seen in zircons extracted from the granite dike of Unit II (03HY5N) (Fig. 3e). The $^{206}Pb/^{238}U$ ages of igneous growth are 157–161 Ma, whereas the inherited core ages range from 680 to 780 Ma. These data suggest that granitic magma was formed by partial melting of metamorphic rocks; some may have metamorphic zircons of 680–780 Ma. The Jurassic intrusive age is coeval with the reported U–Pb SHRIMP zircon age of Kunyushan monzogranite, 160 ± 3 Ma, in the Rushan region (*Hu* et al., 2004) about 35 km to the west (Fig. 1). Numerous post-collisional granitic plutons of 160 Ma occur in the Su–Lu region (e.g., *Guo* et al., 2001) (Fig. 1).

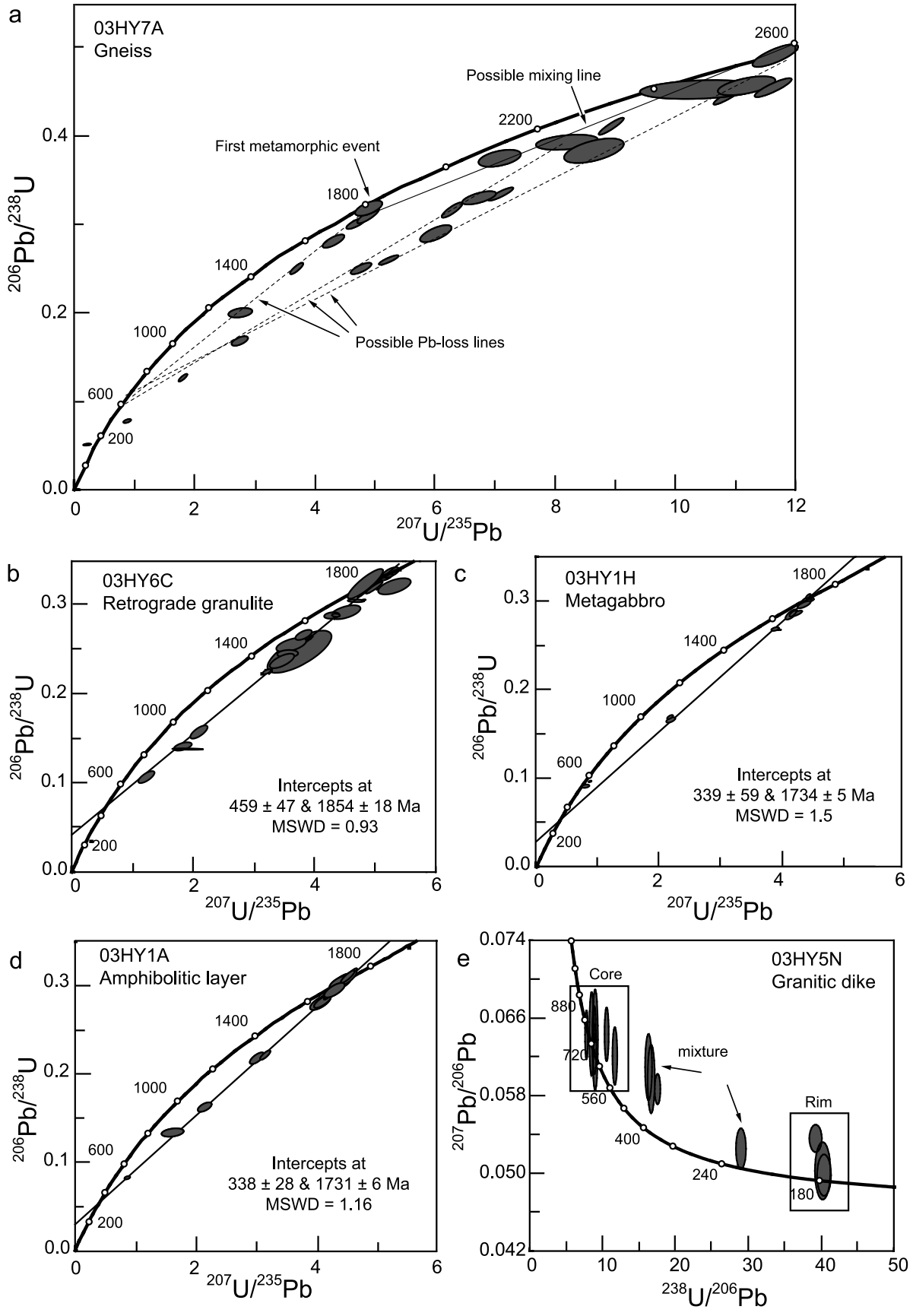
a
03HY7A
Gneiss
Possible mixing line
First metamorphic event
Possible Pb-loss lines
2600
2200
1800
1400
1000
600
200
$^{206}Pb/^{238}U$
$^{207}U/^{235}Pb$
b
03HY6C
Retrograde granulite
Intercepts at
459 ± 47 & 1854 ± 18 Ma
MSWD = 0.93
c
03HY1H
Metagabbro
Intercepts at
339 ± 59 & 1734 ± 5 Ma
MSWD = 1.5
d
03HY1A
Amphibolitic layer
Intercepts at
338 ± 28 & 1731 ± 6 Ma
MSWD = 1.16
e
03HY5N
Granitic dike
Core
mixture
Rim
880
720
560
400
240
180
$^{207}Pb/^{206}Pb$
$^{238}U/^{206}Pb$

Some spots also yielded discordant 218–580 Ma ages. However, CL images revealed that most of these spots are on the boundaries between core and rim, representing the mixtures of igneous and metamorphic ages (Fig. 5). Triassic ages of 220–240 Ma were not obtained for the granitic dike.

Discussion

The Haiyangsuo Complex is exotic to the Sulu terrane

The Sulu terrane consists of the fault-bounded coesite eclogite UHP belt and the eclogite-free HP belt in southern Sulu (e.g., *Zhang* et al., 1994; *Liu* et al., 2004). The rock association and metamorphic evolution of the HYC documented by *Zhang* et al. (2006) and the present paper are different from Sulu UHP and HP rocks. *Ye* et al. (1999) correlated the Haiyangsuo "transitional eclogite" with the "cold eclogite" of south Dabie, and interpreted the HYC as an equivalent to the Dabie "cold eclogite belt". Widespread quartz eclogite in the Dabie Mountains, especially in the Hong'an block, occurs to the south of the coesite-bearing eclogite belt, and has been considered to be "the cold eclogite belt" (e.g., *Eide* and *Liou*, 2000).

However, *Zhang* et al. (2006) revealed two distinct periods of metamorphic recrystallization for the HYC; early HP granulite- to amphibolite-facies metamorphism and later amphibolite-facies overprint. The relict HP granulite assemblages ($Grt + Opx + Cpx + Pl + Hbl \pm Bi \pm Qtz$) formed at $>750\,^{\circ}C$ and 0.9–1.1 GPa and were overprinted by amphibolite-facies phases characterized by well-developed corona layers of Grt and $Hbl + Qtz$; these textures indicate a near-isobaric cooling history of the granulite-bearing gneissic terrane. Metagabbro preserves a relict igneous assemblage in the intrusive core, but has metamorphic corona texture similar to that in granulite; garnet amphibolite at the margins was recrystallized at $\sim$600–700 °C and 0.7–1.0 GPa. The *P–T* paths established for the mafic rocks from the HYC together with the lack of eclogitic assemblages suggest that the Haiyangsuo granulite-amphibolite-gneiss complex has not been subjected to Triassic subduction-zone metamorphism, hence this complex is different from Sulu-Dabie UHP-HP rocks.

Considering our new geochronology, the first HP granulite- to amphibolite-facies metamorphic event occurred at around 1800 Ma and second regional amphibolite-facies overprinting happened around 340–370 Ma, which is supported by the lower-intercept ages of zircons from granulite, metagabbro and an amphibolitic layer. This younger metamorphic event recrystallized most mafic rocks in this region to the amphibolite-facies assemblage of $Hbl \pm Grt + Zo/Czo + Pl + Qtz$. Based on our new age data described above and the previous geochronologic data by *Li* et al. (1994) and *Zhang* et al. (2006), there is no geochronologic evidence of a Triassic metamorphic event at 210–230 Ma, nor 650–850 Ma ages of protoliths common for Sulu UHP/HP rocks, except Neoproterozoic inherited ages from post-collisional Jurassic granitic dikes.

Fig. 5. U–Pb SHRIMP analyses of zircons from the Haiyangsuo Complex. Data are plotted on concordia diagram ($^{206}Pb/^{238}U$ versus $^{207}Pb/^{235}U$) except for granitic dike that uses a Tera-Wasserburg diagram ($^{207}Pb/^{206}Pb$ versus $^{238}U/^{206}Pb$). Errors are 1 sigma. For explanation see text

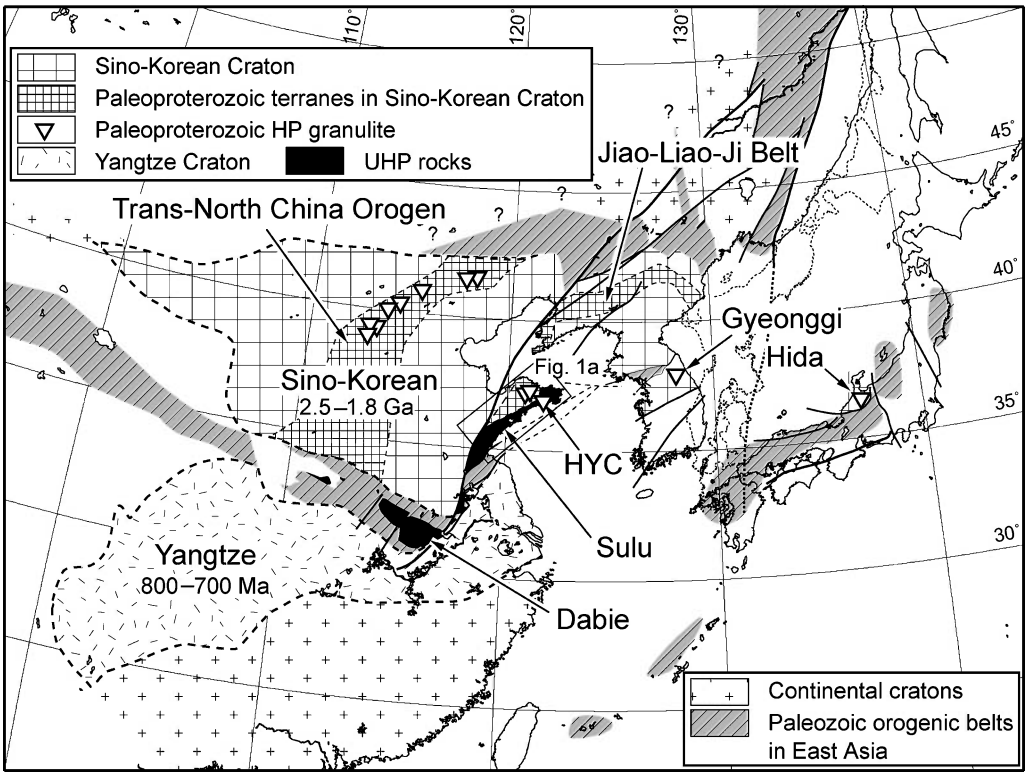

Fig. 6. Simplified geologic map of eastern Asia, showing tectonic correlation between the Haiyangsuo Complex and other Paleoproterozoic HP granulite localities in eastern China, Korean Peninsula and western Japan. Map is modified after *Tsujimori* and *Liou* (2005) and *Zhao* et al. (2004)

Tectonic implications

Where does the HYC fit and correlate with petrotectonic units in NE China and the Korean Peninsula? The geochronological and petrological facts indicate that the HYC is exotic to the Dabie-Sulu UHP-HP terrane. The Archean protolith age of gneissic rocks suggests that this region may be genetically related to the Sino-Korean craton (*Wilde* et al., 2004; *Zhao* et al., 2004, 2005; *Zhai*, 2002, 2004) (Fig. 6). In addition, the HYC also records 1.7–1.85 Ga metamorphic events with mafic intrusions; such Paleoproterozoic metamorphic and igneous events occurred in the Sino-Korean craton. The Trans-North China Orogen has been considered to be the largest Paleoproterozoic metamorphic terrane resulting from a Paleoproterozoic collision between the Western and Eastern Blocks of the Sino-Korean Craton (*Zhao* et al., 2004, 2005) (Fig. 6). This terrane consists of tonalite–trondhjemite–granodiorite (TTG), gneiss, granite-greenstone, and granulite; some granulites have petrologic features and metamorphic ages similar to the HYC granulite (*Zhang* et al., 2006; this study) in spite of more than 800 km separation from the HYC. Another Paleoproterozoic terrane, the Jiao-Liao-Ji Belt, occurs at the northwestern part of the Shandong Peninsula and consists mainly of Late Archean to Paleoproterozoic gneissose and igneous rocks with rare HP granulite-facies rocks (Fig. 6)

(*Zhai* et al., 2000; *Faure* et al., 2003; *Zhao* et al., 2005). The Jiao-Liao-Ji Belt has been thought of as a Paleoproterozoic rift system (*Zhao* et al., 2005) or a continental arc-continent collisional zone (*Bai* and *Dai*, 1998; *Hacker* et al., in press). Considering available petrotectonic information together with petrologic and geochronologic similarities and geography, the HYC may originally be part of the Paleoproterozoic metamorphic terrane developed at the eastern margin of the Sino-Korean craton; the HYC moved and displaced into the northeastern part of the Sulu UHP terrane. Given the fact that no Triassic ages of the Sulu UHP-HP terrane are recorded in the HYC, this tectonic transport must have occurred after the Triassic collision between the Yangtze and Sino-Korean cratons. However, the ∼160 Ma age of granites in both the Haiyangsuo and Rushan regions within 50 km distance indicate that the HYC exotic terrane was juxtaposed to the Sulu UHP terrane by mid-Jurassic time.

Where does the HYC extend to the Korean Peninsula? Paleoproterozoic HP granulites (1.88–1.86 Ga) of the Gyeonggi Massif (*Lee* et al., 2000; *Lee* and *Cho*, 2003; *Cho* et al., 2004) contain Paleoproterozoic zircons with rare Archean inherited cores (2.5–2.0 Ga SHRIMP U–Pb) (*Cho* et al., 2004). Furthermore, zircon SHRIMP geochronology of gneiss from the Hida Belt of SW Japan confirmed the Sino-Korean affinity including both Archean (2.7–2.5 Ga) and Paleoproterozoic (1.84 Ga) events (*Sano* et al., 2000). Rare mafic HP granulites and abundant Jurassic granitic intrusions have been documented in the Hida Belt (*Kunugiza* et al., 2001). The eastern limb of the Sulu UHP terrane has been suggested to extend across the Korean Peninsula eastward to SW Japan (*Ernst* and *Liou*, 1995; *Isozaki*, 1997; *Ishiwatari* and *Tsujimori*, 2003; *Tsujimori* and *Liou*, 2005; *Tsujimori* et al., 2006). We postulate a similar geotectonic configuration for the Archean-Paleoproterozoic granulite-bearing terrane. The Paleoproterozoic HP granulite-bearing terrane including the HYC may be continuous from the present Shandong Peninsula through Yellow Sea northeastward to the Korean Peninsula and SW Japan. Systematic petrologic and geochronologic correlations among these terranes in eastern China, the Korean Peninsula and SW Japan are needed to confirm this suggestion.

Acknowledgments

The authors acknowledge support by the National Science Foundation through grants EAR-0003355 and EAR-0506901 (Liou). This research was also supported by the Stanford McGee Grant and GSA student-research grant to Chu, and the Japanese Society for the Promotion of Science through Research Fellowship for Research Abroad for Tsujimori. We thank Ye Kai, Wang Qingchen, Li Tain-fu and Chen Shi-zong for assistance for our field work, Ruixuan Zhao for SHRIMP analyses and Chris Mattinson, Moon-sup Cho, Jane Gilotti, Takeo Hirajima and Alexander Proyer for detailed review of the manuscript.

References

Bai J, Dai FY (1998) Archean crust of China. In: *Ma XY, Dai FY* (eds) Precambrian crust evolution of China. Springer-Geological Publ. House, Beijing, pp 15–86

Black LP, Kamo SL, Allen CM, Davis DW, Aleinikoff JN, Valley JW, Mundil R, Campbell IH, Korsch RJ, Williams IS, Foudoulis C (2004) Improved $^{206}Pb/^{238}U$ microprobe geochro-

nology by the monitoring of a trace-element-related matrix effect: SHRIMP, ID-TIMS, ELA-ICP-MS and oxygen isotope documentation for a series of zircon standards. Chem Geol 205: 115–140

Cho M, Kim HC, Kim JH, Wan YS, Liu D (2004) Geochronologic correlation between the Gyeonggi Massif, Korea, and the South China Craton: Evidence from the SHRIMP U–Pb zircon ages. In: Asia Oceania Geosciences Soc 1st Ann Meet, Abstract, Singapore, pp 69

Chu W (2005) Geochronological and petrological studies of Haiyangsuo region, Sulu UHP terrane, eastern China. Stanford Univ Master's thesis, Stanford, 82 pp

Dong SW, Oberhänsli R, Schmidt R, Liu XC, Tang JF, Xue HM (2002) Occurrence of metastable rocks in deeply subducted continental crust from the Dabie Mountains, central China. Episodes 25: 84–89

Eide E, Liou JG (2000) High-pressure blueschists and eclogites in Hong'an: a framework for addressing the evolution of ultrahigh-pressure rocks in central China. Lithos 52: 1–22

Ernst WG, Liou JG (1995) Contrasting plate-tectonic styles of the Qinling-Dabie-Sulu and Franciscan metamorphic belts. Geology 23: 353–356

Faure M, Lin W, Monié P, Le Breton N, Poussineau S, Panis D, Deloule E (2003) Exhumation tectonics of the ultrahigh-pressure metamorphic rocks in the Qinling orogen in east China: New petrological-structural-radiometric insights from the Shandong Peninsula. Tectonics 22: DOI: 10.1029/2002TC001450

Guo JH, Chen F, Zhang X, Fan HR, Cong BL (2001) Origin of post-collisional shoshonitic syenites and strongly peraluminous rocks in Sulu UHP belt, eastern China: Zircon U–Pb and petrologic-chemical data. In: *Jang BA, Dekyo Cheong* (eds) Proceeding of the 8th Korea-China joint symposium on crustal evolution in Northeast Asia. Kongwon National University, Kyunju, South Korea, pp 126–129

Hacker BR, Ratschbacher L, Webb L, McWilliams MO, Ireland T, Calvet A, Dong S, Wenk HR, Chateigner D (2000) Exhumation of ultrahigh-pressure continental crust in east central China. J Geophys Res 105: 13339–13364

Hacker BR, Wallis S, Ratschbacher L, Grove M, Gehrels G (in press) U–Pb SIMS and LA-ICP-MS zircon and monazite ages constrain ultrahigh-pressure metamorphism and the architecture of the ultrahigh-pressure Sulu orogen. Tectonics

Hirajima T, Nakamura D (2003) The Dabie Shan-Sulu orogen. In: *Carswell DA, Compagnoni R* (eds) Ultrahigh-pressure metamorphism. EMU Notes in Mineralogy 5: 105–144

Hirajima T, Wallis S, Zhai M, Ye K (1993) Eclogitized metagranitoid from the Su–Lu ultrahigh-pressure (UHP) province, eastern China. Proc Japan Acad 69B: 249–253

Hu F, Fang H, Yang J, Wan Y, Liu D, Zhai M, Jin C (2004) Mineralizing age of the Rushan Iode gold deposit in the Jiaodong Peninsula; SHRIMP U–Pb dating on hydrothermal zircon. Chinese Sci Bull 49: 1629–1636

Ishiwatari A, Tsujimori T (2003) Paleozoic ophiolites and blueschists in Japan and Russian Primorye in the tectonic framework of East Asia: a synthesis. Island Arc 12: 190–206

Isozaki Y (1997) Contrasting two types of orogen in Permo-Triassic Japan: Accretionary versus collisional. Island Arc 6: 2–24

Jahn BM, Rumble D, Liou JG (2003) Geochemistry and isotope tracer study of UHPM rocks. In: *Carswell DA, Compagnoni R* (eds) Ultrahigh-Pressure Metamorphism. EMU Notes in Mineralogy 5: 365–414

Kretz R (1983) Symbols for rock-forming minerals. Am Mineral 68: 277–279

Kunugiza K, Tsujimori T, Kano T (2001) Developments of the Hida and Hida marginal belts. In: *Kano T* (ed) ISRGA field guidebook for major geologic units of Southwest Japan – excursion guidebook for the field workshop of international symposium on the assembly and breakup of Rodinia and Gondwana, and growth of Asia, pp 75–131

Lee SR, Cho M (2003) Metamorphic and tectonic evolution of the Hwacheon granulite complex, central Korea: composite P–T path resulting from two district crustal-thickening events. J Petrol 44: 197–225

Lee SR, Cho M, Yi K, Stern R (2000) Early Proterozoic granulites in central Korea: tectonic correlation with Chinese cratons. J Geol 108: 729–738

Li S, Chen Y, Song Z, Zhang Z, Yang C, Zhao D (1994) U–Pb zircon ages of amphibolite from the Haiyangsuo area, Eastern Shandong Province – An example for influence of multi metamorphism to lower and upper intercepts of zircon discordia line at the concordia curve. Acta Geoscientia Sinica 37: 37–42

Liou JG, Zhang RY, Jahn BM (1997a) Petrology, geochemistry and isotope data on a ultrahigh-pressure jadeite quartzite from Shuanghe, Dabie Mountains, east-central China. Lithos 41: 59–78

Liou JG, Zhang RY, Maruyama S (1997b) Lack of eclogite precursor for a garnet amphibolite in the NE Sulu UHP terrane, eastern China. In: Fifth International Eclogite Conference. Terra Nova Abstract Supplement 1, Blackwell Science, p 18

Liu F, Xu Z, Liou JG, Katayama I, Masago H, Maruyama S, Yang J (2002) Ultrahigh-P mineral inclusions in zircons from gneissic core samples of the Chinese continental scientific drilling site in eastern China. Eur J Mineral 14: 499–512

Liu F, Xu Z, Liou JG, Song B (2004) SHRIMP U–Pb ages of ultrahigh-pressure and retrograde metamorphism of gneissic rocks, southwestern Sulu terrane, eastern China. J Metamorph Geol 22: 315–326

Liu F, Liou JG, Xu Z, Liang F (in press) Identification of UHP and non-UHP orthogneisses in the Sulu UHP terrane (eastern China): Evidences from SHRIMP U–Pb dating on mineral inclusion-bearing zircons. Intl Geol Rev

Ludwig KR (2001) SQUID 1.02. Berkeley Geochronology Center Special Publ No. 2

Ludwig KR (2003) Isoplot 3. Berkeley Geochronology Center Spec Publ No. 4

Oberhänsli R, Martinotti G, Schmidt R, Liu X (2002) Preservation of primary volcanic textures in the ultrahigh-pressure terrain of Dabie Shan. Geology 30: 699–702

Regional Geology of Shandong Province (1991) People's republic of China Ministry of Geology and Mineral Resources, Geological memoirs, series 1 no. 26. Geol Publishing House, Beijing

Rumble D, Liou JG, Jahn BM (2003) Continental crust subduction and UHP metamorphism. In: *Rudnick RL* (ed) The crust, 3 – *Holland HD, Turekian KK* (eds) Treatise on geochemistry, Elsevier, Oxford, pp 293–319

Sano Y, Hidaka H, Terada K, Shimizu H, Suzuki M (2000) Ion microprobe U–Pb zircon geochronology of the Hida gneiss: Finding of the oldest minerals in Japan. Geochem J 34: 135–153

Schmidt R, Romer RL, Franz L, Oberhänsli R, Martinotti G (2003) Basement-cover sequences within the UHP unit of the Dabie Shan. J Metamorph Geol 21: 531–538

Tsujimori T, Liou JG (2005) Eclogite-facies mineral inclusions in clinozoisite from Paleozoic blueschist, central Chugoku Mountains, SW Japan: Evidence of regional eclogite-facies metamorphism. Intl Geol Rev 47: 215–232

Tsujimori T, Liou JG, Ernst WG, Itaya T (2006) Triassic paragonite- and garnet-bearing epidote-amphibolite from the Hida Mountains, Japan. Gondwana Res 9: 167–175

Wallis S, Tsuboi M, Suzuki K, Fanning M, Jiang L, Tanaka T (2005) Role of partial melting in the evolution of the Sulu (eastern China) ultrahigh-pressure terrane. Geology 33: 129–132

Wang X, Liou JG (1991) Regional ultrahigh-pressure metamorphic terrane in central China: Evidence from coesite-bearing eclogite, marble, and metapelite. Geology 19: 933–936

Wilde SA, Cawood PA, Wang K, Nemchin A, Zhao G (2004) Determining Precambrian crustal evolution in China: a case-study from Wutaishan, Shanxi Province, demonstrating the application of precise SHRIMP U–Pb geochronology. In: *Malpas J, Fletcher CJN, Ali JR, Aitchison JC* (eds) Aspects of the tectonics evolution of China. Geol Soc London, Special Publ 226: 27–55

Williams IS (1998) U–Th–Pb geochronology by ion microprobe. In: *Mickibbeen MA, Shanks III WC, Ridley I* (eds) Application of microanalytical techniques to understanding mineralizing processes. Rev Econ Geol 7: 1–35

Yang JS, Wooden JL, Wu CL, Liu FL, Xu ZQ, Shi RD, Katayama I, Liou JG, Maruyama S (2003) SHRIMP U–Pb dating of coesite-bearing zircon from the ultrahigh-pressure metamorphic rocks, Sulu terrane, east China. J Metamorph Geol 21: 551–560

Ye K, Cong B, Hirajima T, Banno S (1999) Transformation from granulite to transitional eclogite at Haiyangsuo, Rushan County, eastern Shandong Peninsula: The kinetic process and tectonic implications. Acta Petrologica Sinica 15: 21–36 (in Chinese with English abstract)

Zhai M (2002) Where is the North China–South China block boundary in eastern China? Comment and reply. Geology 30: 667–667

Zhai M (2004) Precambrian tectonic evolution of the North China Craton. In: *Malpas J, Fletcher CJN, Ali JR, Aitchison JC* (eds) Aspects of the tectonics evolution of China. Geol Soc London, Special Publ 226: 57–72

Zhai M, Cong B, Guo J, Liu W, Li Y, Wang Q (2000) Sm–Nd geochronology and petrography of garnet pyroxene granulites in the northern Sulu region of China and their geotectonic interpretation. Lithos 52: 23–33

Zhang RY, Liou JG (1997) Partial transformation of gabbro to coesite-bearing eclogite from Yangkou, the Sulu terrane, eastern China. J Metamorph Geol 15: 183–202

Zhang RY, Liou JG, Cong B (1994) Petrogenesis of garnet-bearing ultramafic rocks and associated eclogites in the Su–Lu UHP metamorphic terrane, eastern China. J Metamorph Geol 12: 169–186

Zhang RY, Liou JG, Tsujimori T, Maruyama S (2006) Non-UHP unit bordering the Sulu UHP terrane, eastern China: Transformation of proterozoic granulite and gabbro to garnet amphibolite. In: *Hacker BR, McClelland W, Liou JG* (eds) Ultrahigh-pressure metamorphism: Deep continental subduction. Geol Soc Am Spec Paper 403: 169–207

Zhao G, Sun M, Wilde SA, Guo J (2004) Late Archean to Paleoproterozoic evolution of the Trans-North China Orogen: insights from synthesis of existing data from the Hengshan–Wutai–Fuping belt. In: *Malpas J, Fletcher CJN, Ali JR, Aitchison JC* (eds) Aspects of the tectonics evolution of China. Geol Soc London Spec Publ 226: 27–55

Zhao G, Sun M, Wilde SA, Li S (2005) Late Archean to Paleoproterozoic evolution of the North China Craton: key issues revisited: Precambrian Res 136: 177–202

Zheng YF, Fu B, Gong B, Li L (2003) Stable isotope geochemistry of ultrahigh pressure metamorphic rocks from the Dabie-Sulu orogen in China: implications for geodynamics and fluid regime. Earth Sci Rev 62: 105–161

Authors' addresses: *J. G. Liou* (corresponding author; e-mail: liou@pangea.stanford.edu), *T. Tsujimori, W. Chu, R. Y. Zhang*, Department of Geological and Environmental Sciences, Stanford University, Stanford, California 94305, U.S.A.; *J. L. Wooden*, U.S. Geological Survey, 345 Middlefield Road, Menlo Park, California 94025, U.S.A.